Letter

# Curvature-driven ac-assisted creep dynamics of magnetic domain walls

P. Domenichini,[1,2] F. Paris,[3] M. G. Capeluto,[1,2] M. Granada,[4,5] J.-M. George,[6] G. Pasquini,[1,2] and A. B. Kolton[3,5]

[1]*Universidad de Buenos Aires, FCEyN, Departamento de Física, 1428 Buenos Aires, Argentina*

[2]*CONICET-Universidad de Buenos Aires, IFIBA, 1428 Buenos Aires, Argentina*

[3]*Centro Atómico Bariloche, CNEA, CONICET, R8402AGP Bariloche, Argentina*

[4]*Instituto de Nanociencia y Nanotecnología, CNEA–CONICET, Centro Atómico Bariloche, (R8402AGP) San Carlos de Bariloche, Río Negro, Argentina*

[5]*Instituto Balseiro, Universidad Nacional de Cuyo, R8402AGP Bariloche, Argentina*

[6]*Unité Mixte de Physique, CNRS, Thales, Université Paris-Sud, Université Paris-Saclay, Palaiseau F-91767, France*

(Received 16 December 2020; revised 27 April 2021; accepted 9 June 2021; published 24 June 2021)

The dynamics of micrometer-sized magnetic domains in ultrathin ferromagnetic films is so dramatically slowed down by quenched disorder that the spontaneous elastic tension collapse becomes unobservable at ambient temperature. By magneto-optical imaging we show that a weak zero-bias ac magnetic field can assist such curvature-driven collapse, making the area of a bubble to reduce at a measurable rate, in spite of the negligible effect that the same curvature has on the average creep motion driven by a comparable dc field. An analytical model explains this phenomenon quantitatively.

DOI: 10.1103/PhysRevB.103.L220409

An arbitrarily weak quenched disorder has yet a notable qualitative effect on the driven motion of an extended elastic system such as an interface embedded in a random medium. A paradigmatic experimental example is pinned domain walls (DWs) in thin film "Ising-like" ferromagnets with a uniform external magnetic field favoring the growth of a magnetic domain [1–3]. In these materials, due to the practically unavoidable presence of random heterogeneities, DW velocities can vary dramatically under relatively modest changes of a weak applied field. Strikingly, the quantitative way the velocity asymptotically vanishes in the small field limit is *universal* [4–6], and is thus succesfully captured by minimal models that can be solved, in the limit of large systems, with powerful analytical [7] and numerical [8–11] techniques. These statistical-physics models yield, in particular, the celebrated creep-law $\ln(1/v) \propto H^{-\mu}$ for the average velocity $v$ of a DW in the presence of weak uniform magnetic driving field $H$, with $\mu > 0$ a universal exponent [4,5,12]. This law clearly signals the breakdown of linear response in the collective transport. The success of this mathematical description unveils the basic physics fact that the glassy universal dynamics of DWs is mainly controlled by the interplay of pinning, elasticity, and thermal fluctuations on the driven elastic interface. As such, creep theory is relevant for many other driven elastic systems with thermal or "thermal-like" fluctuations and quenched disorder, ranging from ferroelectric domain walls [13–17], current driven vortices in superconductors [18–22], charge density waves [23], to tension driven cracks [24,25].

Many universal properties predicted by the creep theory, the velocity-force characteristics [4,5,7,12], the rough geometry of moving DWs [8–10], and even the event statistics behind the creep law [11,26], have been studied experimentally by applying external magnetic fields [1,2,6,27–33] or external currents [34–38] to drive DWs in ultrathin ferromagnetic films with perpendicular magnetic anysotropy (PMA). Most of the studies focus on the dc-driven case while comparatively very few experimental [14,33] and theoretical [39,40] studies have focused on the *universal* properties that can emerge under a zero-bias ac drive within the creep regime. Weak ac fields yield nevertheless a rich phenomenology which is worth studying. In particular, recent experiments have shown that roughly circular magnetic bubbles evolve under a pure symmetric ac field in a very intriguing way [33]. The first interesting effect is that the (otherwise ultrastable) initial bubble monotonically shrinks with the number of alternated positive and negative magnetic field pulses of equal strength, apparently "rectifying" the ac drive. The second is the observation that the DW roughness increases at a much faster rate in the ac protocol compared to the dc for the same amplitude of the drive. An example of such evolution, captured by successive MO images, is shown in Fig. 1. These two intriguing effects have not been explained yet.

In this article we show that the elastic pressure arising from the domain mean curvature, even being orders of magnitude weaker than the driving field pressure, is responsible for the shrinking of the domain area under ac fields. To show this, we first derive a model for the ac-driven DW dynamics and second, we quantitatively test two of its predictions experimentally: (i) the pulse asymmetry needed to stabilize the average size of the "beating domain" and (ii) the area collapse rate in the initial dynamics for the case of symmetric positive-negative pulses. Finally, a qualitative argument is given to explain the ac enhancement of the DW dynamic roughening and its effect on the area collapse dynamics.

 

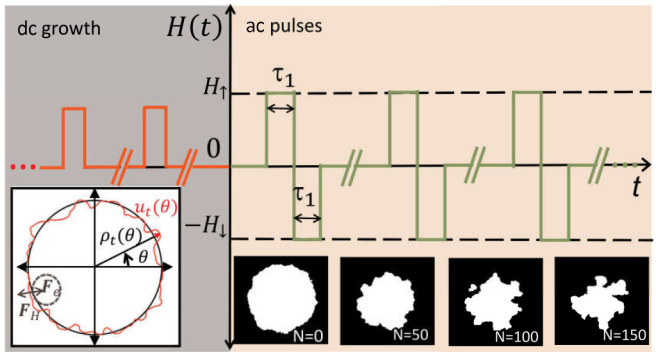


FIG. 1. Schematics of the magnetic field protocol. Pulses applied to grow the domain (red) are followed by the ac-driving pulses (green) with amplitudes $H_\uparrow$ and $-H_\downarrow$. The sequence of PMOKE images in the bottom corresponds to the case $H_\uparrow = H_\downarrow$ for an increasing number $N$ of pulses. (Inset) Diagram of the contour $\Gamma_t$ of a typical domain at an arbitrary time $t$, where $u_t(\theta)$ indicates the domain profile measured from the average radius $\rho_t(\theta)$. $\mathbf{F}_e$ and $\mathbf{F}_H$ are the elastic and field normal forces per unit length, respectively.

The proposed model is very simple. Let us consider a segment of a thin DW in a film of thickness $d$. In the absence of disorder and thermal fluctuations, the total force $\mathbf{F}$ per unit length acting on the effectively one-dimensional (1D) DW is the sum of the magnetic field force $\mathbf{F}_H = 2M_s dH\hat{n}$ and the elastic force $\mathbf{F}_e = \sigma d\kappa\hat{n}$, with $M_s$ being the saturation magnetization, $\sigma$ the DW surface tension, and $\kappa$ the DW signed local curvature. Both forces are parallel to the DW local outward normal $\hat{n}$ (see inset in Fig. 1). For instance, for a perfectly circular bubble of radius $R$, the "Young-Laplace" effective magnetic field $C\kappa \approx -C/R$, with the constant $C = \sigma/2M_s$, opposes domain growth. Assuming an overdamped dynamics we have $\dot{R} = m(H - C/R)$, with $m$ the effective DW mobility. For $H = 0$ this predicts the linear decay $A_t = A_0 - (2\pi Cm)t$, where $A_t \equiv \pi R_t^2$ is the shrinking circle area. The bubble is hence unstable and its lifetime scales as $\sim A_0$. This result can be also obtained from the general Allen-Cahn equation [41]. Quite remarkably the result actually holds for *any* simple time-dependent closed curve $\Gamma_t$ [42] for which we can write

$$\frac{dA_t}{dt} = \int_{\Gamma_t} v_t(\mathbf{r}_s)ds, \tag{1}$$

with $v_t(\mathbf{r}_s)$ the local instantaneous normal velocity at point $\mathbf{r}_s$ in $\Gamma_t$. If we assume a linear and instantaneous response $v_t(\mathbf{r}_s) = m[H_t + C\kappa_t(\mathbf{r}_s)]$, with $\kappa_t(\mathbf{r}_s)$ the instantaneous signed local curvature we easily obtain, using the topological index of the curve $\int_{\Gamma_t}\kappa_t(\mathbf{r}_s)ds = -2\pi$, the rate $\frac{dA_t}{dt} = mH_tP_t - 2\pi Cm$, with $P_t \equiv \int_{\Gamma_t} ds$ the perimeter. This generalizes the $H_t = 0$ constant decay rate $\frac{dA_t}{dt} = -2\pi Cm$ to *any* initial simple closed curve $\Gamma_t$.

In the presence of quenched and thermal disorder the above results are not valid as the normal velocity $v_t(\mathbf{r}_s)$ is in general expected to be an inhomogeneous nonlinear function of $H_t + C\kappa_t$. Assuming again instantaneous response we can write Eq. (1) as

$$\frac{dA}{dt} \approx \int_{\Gamma_t} V_T(H_t + C\kappa_t(\mathbf{r}_s), \mathbf{r}_s)ds, \tag{2}$$

with $V_T(h, \mathbf{r})$ a temperature- and position-dependent velocity response function evaluated at the local field $h_t = H_t + C\kappa_t$. We will argue that for weak enough fields, $V_T(h, \mathbf{r})$ in Eq. (2) can be approximated by the well-known creep law for dc-driven DWs. This hydrodynamic approach can be formally justified: in the creep regime, DW velocity is mainly controlled by creep events with a cutoff radius estimated to be, for ultrathin ferromagnets, less than 0.1 $\mu$m [11,31], clearly well below the $\sim$1-$\mu$m PMOKE resolution. Therefore, larger size fluctuations are expected to introduce only negligible logarithmic corrections [10] into the creep law $V_T(h) \sim \exp[-(T_d/T)(H_d/h)^\mu]$ that describes the DW velocity in terms of the effective field $h$, temperature $T$, and also the disorder and elasticity through $T_d$, and $H_d$ [43]. Similarly, the characteristic time associated with individual creep events is much smaller than the experimental time scale used for resolving DW displacements so the velocity response can be considered local and instantaneous.

Replacing the creep velocity $V_T(h_t, \mathbf{r})$ in Eq. (2) is a step forward but still yields a nonclosed equation for $dA_t/dt$ as it requires the knowledge of the time-dependent curvature field $\kappa_t(\mathbf{r})$, together with a model for the spatially fluctuating pinning parameters of the creep law. Nevertheless, to extract the basic physics some progress can be made by first making the well-justified approximation that $H_t \gg C\kappa_t$ [44]. Second, the complexity of Eq. (2) is greatly reduced if we neglect the heterogeneity of the creep law and replace it by its average $V_T(h, \mathbf{r}) \approx V_T(h)$ or velocity-field characteristics. This approximation is not equivalent to neglect disorder completely, as $V_T(h)$ is in general quite different from the $V_T(h) \propto h$ expected for a homogeneous sample, particularly in the strongly nonlinear creep regime. Developing then at first order in $C\kappa_t$ from Eq. (2) we obtain

$$\frac{dA_t}{dt} \approx V_T(H_t)P_t - 2\pi CV_T'(H_t), \tag{3}$$

only relating the geometric variables $A_t$ and $P_t$. The position and time-dependent curvature $\kappa_t(\mathbf{r})$ disappears thanks to the topological invariant $\int_{\Gamma_t}\kappa_t = -2\pi$ [45]. Let us now focus on the experiments and make some concrete predictions with Eq. (3).

Our measurements were carried out in ultrathin ferromagnetic films with PMA, by magneto-optical imaging, using a homemade polar magneto-optical Kerr effect (PMOKE) microscope. Two kinds of samples from different sources were used: a Pt/Co/Pt magnetic monolayer (S1) and a Pt/[Co/Ni]4/Al multilayer (S2), both grown by dc magnetron sputtering [46,47]. Helmholtz coils allow one to apply well-conformed square magnetic field pulses with amplitude $H$ up to 700 Oe and duration $\tau_1 > 1$ ms. DW dynamics is characterized with the usual quasistatic technique (see [45] for experimental details). The ac field is applied to an already grown domain (see Fig. 1) and it consists of alternated square pulses of identical duration $\tau_1$ and amplitude $H = H_\uparrow > 0$ (expanding the domain), and $H = -H_\downarrow < 0$ (compressing the domain). The two pulses are periodically repeated with period $\tau \geqslant 2\tau_1$, as schematized in Fig. 1. The magnitudes of all applied fields are such that the creep law with $\mu = 1/4$ is well observed in the dc protocol (see [45]).

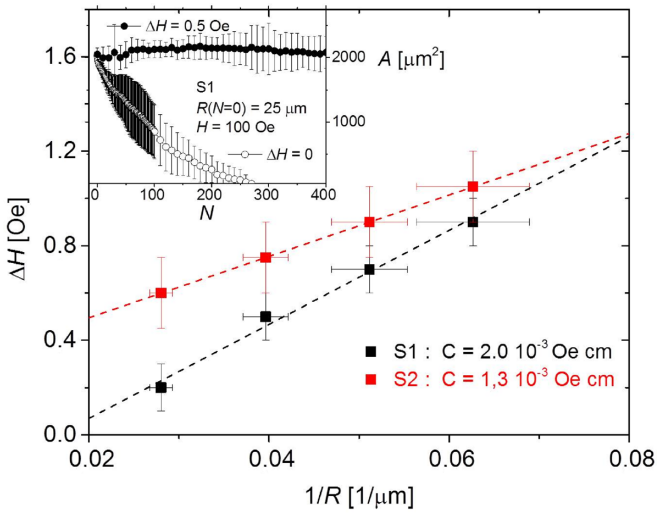


FIG. 2. Field pulse asymmetry $\Delta H$ used to compensate the curvature collapse of domains with different initial radii $R$. (Inset) Evolution of the domain area $A$ with the pulse number, for symmetric pulses $\Delta H = 0$ and for nearly compensating asymmetric pulses $\Delta H = 0.5$ Oe.

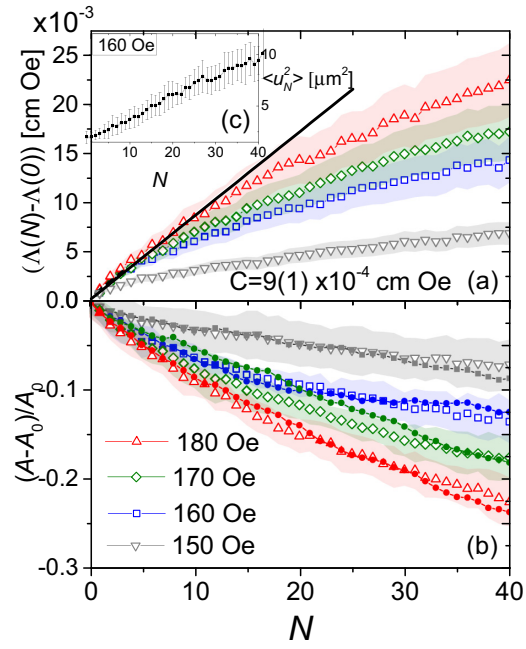


FIG. 3. Open symbols and dashed regions show the evolution of the mean value and statistical variance of $\Lambda(N)$ (see text) (a) and of the relative domain area change $\Delta A/A_0$ (b), for different amplitudes of symmetric pulses in sample S2. The black line in (a) is a linear fit of the initial evolution of $\Lambda(N)$ with $H$ ranging from 160 to 180 Oe, yielding the micromagnetic constant $C$. In (b) numerical simulation results are shown with full symbols. Inset (c) shows DW mean squared displacements for $H = 160$ Oe pulses.

Since we are only interested in the smooth evolution of $A_t$ and $P_t$ as a function of the number $N$ of ac cycles we define $\mathcal{A}$ and $\mathcal{P}$ such that $d\mathcal{A}/dN \equiv A_{n+1} - A_n$ and $d\mathcal{P}/dN \equiv P_{n+1} - P_n$, where $n \equiv t/\tau$. Integrating Eq. (3) from $t = n\tau$ to $t = (n+1)\tau$ we thus obtain

$$\frac{d\mathcal{A}}{dN} \approx -2\pi C V_T'(H_\uparrow)\tau - \frac{\tau}{4} V_T(H_\uparrow)\frac{d\mathcal{P}}{dN} + \frac{\tau}{2}\Delta H V_T'(H_\uparrow)\mathcal{P}, \tag{4}$$

where $\Delta H = H_\uparrow - H_\downarrow \ll H_\uparrow$ quantifies a possible pulse asymmetry, and we have used the expected symmetry $V_T(h) = -V_T(-h)$.

We test Eq. (4) in two different ways. On one hand, we can choose $\Delta H = \Delta H^*$ such that $d\mathcal{A}/dN = d\mathcal{P}/dN = 0$,

$$\Delta H^* = \frac{2C}{\mathcal{R}}, \tag{5}$$

where we have defined $\mathcal{R} \equiv \mathcal{P}/2\pi$, approximately the observed average domain radius. This is a simple but rather general prediction: $\Delta H^*$ is independent of $V_T$ only provided that $V_T(h) = -V_T(-h)$, and of the ac parameters $\tau$ and $H_\uparrow$. In physical terms, Eq. (5) states that even weak compressing forces arising from mean curvature are relevant because they *break the forward-backward symmetry* of the DW velocity in the ac field. Importantly, Eq. (5) connects with micromagnetism through $C = \sigma/2M_s$. Using that $\mathcal{A}_N \approx A_N$, in Fig. 2 we test Eq. (5) experimentally. The main panel shows the field asymmetry $\Delta H$ stabilizing the average area $A$ of initially nucleated domains with different initial radius $R$. An example of such compensation is shown in the inset, where the evolution of $\mathcal{A}(N)$ under symmetric field pulses and asymmetric compensating pulses are compared for sample S1, with an initial $R = 25\mu$m. For both samples, there is a good agreement with the linear relation between $\Delta H^*$ and $1/\mathcal{R}$ predicted in Eq. (5), for four $R$ values ranging from 15 $\mu$m to 35 $\mu$m. The ordinates, predicted to be zero in Eq. (5), are compatible with a small spurious dc field present in the laboratory. The fitted value of $C$ is in both cases of order $10^{-3}$Oe cm, fairly agreeing with $C_{S1} = 2.1 \times 10^{-3}$ Oe cm and $C_{S2} = 1.2 \times 10^{-3}$ Oe cm estimated as $C = \sigma/2M_s$ from the micromagnetic parameters, respectively [45].

Let us now go further and focus on the interesting case of symmetric field pulses $H_\uparrow = H_\downarrow = H$, i.e., $\Delta H = 0$. From Eq. (4) we simply predict

$$-\frac{d}{dN}\left[\frac{\mathcal{A} + \frac{\tau}{4}V_T(H)\mathcal{P}}{2\pi V_T'(H)\tau}\right] = \frac{d\Lambda}{dN} \approx C. \tag{6}$$

For circular DWs with radius $R_t$, this equation can be readily obtained from $dR_t/dt \approx V(H_t + C\kappa_t)$ with $\kappa_t = -1/R_t$. Remarkably, however, Eq. (6) is valid regardless of the circular shape assumption (see [45] for further details) and contains the spontaneous ($H = 0$) collapse as a special case. Figure 3(a) shows the evolution of the function $\Lambda(N)$ defined in Eq. (6), for four different field amplitudes, measured in sample S2. The initial slope for the highest amplitudes, using the creep-regime velocity-field characteristics measured in S2, gives $C \approx 10^{-3}$Oe cm, again in fair agreement with the micromagnetic estimate for $C$, hence reinforcing the curvature argument.

Results shown in Figs. 2 and 3(a) confirm that surface tension forces arising from curvature are responsible for the domain collapse, in spite of being two orders of magnitude smaller than the ac forces. They also validate the proposed model but, as can be appreciated in Fig. 3(a), only for the very first few ac cycles (small $N$). The linear

approximation deviates from the data at smaller $N$ as $H$ decreases. We argue that these deviations are due to large-scale dynamic roughening, neglected in our simple model. To show this we exploit that creep dynamics displays a "depinning-like" regime upon coarse graining many creep events [7–9] and thus numerically emulate the experimental protocol using the time-dependent Ginzburg-Landau model [48–51],

$$\eta\partial_t\phi = c\nabla^2\phi + \epsilon_0[(1 + r(x, y))\phi - \phi^3] + \tilde{h}_t, \qquad (7)$$

near the depinning transition, where $\phi \equiv \phi(x, y, t)$ models the local magnetization, and $r(x, y)$ an uncorrelated random-bond type of disorder of strength $r_0$ [52]. The *effective* ac field $\tilde{h}_t = \pm\tilde{h}_0$ of period $\tilde{\tau}$ is chosen so as to impose a given average displacement of the DW in half a period comparable to that observed in the experiments. After nucleating a circular domain with saturation magnetization $\phi_s \sim 1$, this model generates a closed curve $\Gamma_t$ (i.e., $\phi(\mathbf{r}_s) = 0$ for $\mathbf{r}_s \in \Gamma_t$) describing a DW with width $\delta \sim \sqrt{c/\epsilon_0}$, and surface tension $\sigma \sim \sqrt{c\epsilon_0}$, driven by an ac field in a disordered environment. When $r_0 = 0$, Eq. (6) is very accurately satisfied if we replace $V_T(H)\tau \to \tilde{h}_0\tilde{\tau}\delta/\eta$ and $V_T'(H)\tau \to \tilde{\tau}\delta/\eta$ and $C \to \sqrt{c\epsilon_0}$ [45]. When $r_0 \neq 0$, however, we go beyond the homogeneity assumption and a deviation from Eq. (6) similar to the experiment is found. Strikingly, we can empirically adjust $r_0$, and then tune $\tilde{h}$ and $\tilde{\tau}$ so as to accurately reproduce the experimental data for the different fields, as shown in Fig. 3(b). Large-scale dynamic roughening within the creep regime hence slows down the curvature-driven collapse. The better agreement for small $N$ between the prediction [Eq. (6)] and the experiment [Fig. 3(a)] for increasing ac fields is explained by the smoothing effect of the DW velocity.

Finally, we aim to explain why the ac dynamic roughening discussed above is enhanced with respect to the dc-driven case [33]. As a general fact, we expect that a recently nucleated driven DW will display, as it correlates with the disorder, a growing DW mean squared width, $w_t^2 \sim t^{2\zeta/z}$, with $\zeta$ and $z$ the roughness and dynamic exponents, respectively [53]. If the large-scale geometry of a DW in the dc creep regime is described by the Edwards-Wilkinson (EW) equation with an effective temperature [7,9,31] we expect $z = 2$ and $\zeta = 1/2$, so $w_t^2 \sim t^{1/2}$ for the 1D DW. For the ac case we expect instead a temporally correlated noise since the DW can revisit repetitively the same disorder in its oscillatory motion. If we model such colored noise $\eta(x, t)$ with an exponent $\psi > 0$, such that for two points in a DW segment $\langle\eta(x, t)\eta(x, t')\rangle \sim \delta(x - x')|t - t'|^{2\psi-1}$ ($\psi = 0$ for uncorrelated noise) linear theory predicts $z = 2$ and $\zeta = 1/2 + 2\psi > 1/2$ [53]. Therefore $w_t^2$ should grow *faster* than in the dc case. To test this idea we describe the experimental DW in polar coordinates $\rho(\theta, t)$ [54], and define $u_t(\theta) = \rho_t(\theta) - R_t$ with $R_t \equiv \langle\rho_t(\theta)\rangle$ the angle-averaged radius (see inset in Fig. 1), and then compute the roughness after $N$ cycles $w_N^2 = \langle u_N^2\rangle$. The inset of Fig. 3 shows an example of the ac evolution of $w_N^2$ in sample S2. Interestingly, it can be seen that $w_N^2 \sim N$, faster than the prediction for uncorrelated noise and compatible with correlated noise with $\psi \approx 1/2$ in the relevant $N$ range [55]. This may explain qualitatively why DWs in the ac protocol are rougher than in the dc protocol for identical field amplitude and time window, as observed experimentally [33], and in recent simulations [51].

Summarizing, we have proposed and experimentally tested a model for the DW creep dynamics of an isolated magnetic domain in an ultrathin ferromagnet under ac fields at ambient temperature. We showed that curvature effects, with a negligible effect on the average dc-driven motion, play nevertheless a central role in the ac-driven case. The intriguing "rectification effect" in the zero-bias ac case of Ref. [33] is then explained by the curvature-induced symmetry breaking of forward-backward DW motions. Rather strikingly, the same curvature effects are unable to produce, without ac assistance, any experimentally observable DW displacement [56]. We have also explained, qualitatively, the ac enhancement of large-scale dynamic roughening. A systematic study of temperature dependence could give additional cross-check of the model predictions and further useful insight. Although we have focused on their important role in the ac-assisted motion, curvature effects can be relevant in some dc-driven systems as well: A nonsteady velocity in dc-driven circular domains was experimentally reported [57]; on the other hand, in thin and narrow ferromagnetic wires the universal creep law is satisfied by the dc-driven steady DW velocity only if an effective "counterfield" $\Delta H$ [58,59], proportional to the observed average curvature of the narrow DW, is added, in agreement with our arguments. In the latter case, however, average curvature is not inherited from the initial conditions but steadily maintained by the strong localized "dynamic friction" at the wire edges. Due to the simplicity and generality of our arguments, we hope that the present work will open new perspectives for modeling and controlling DW creep motion in analog ferroelectric materials [15,17,60], as well as in a variety of elastic systems, far beyond ferromagnetic films.

## ACKNOWLEDGMENTS

We especially thank J. Curiale, G. Durin, E. Ferrero, V. Jeudy, and A. Rosso for useful discussions. This work was partially supported by Consejo Nacional de Investigaciones Científicas y Técnicas - Argentina (CONICET), the University of Buenos Aires, and Grants PICT2016-0069 (MinCyT), UNCuyo2019-06/C578, and UBACyT 20020170100496BA.

[1] S. Lemerle, J. Ferré, C. Chappert, V. Mathet, T. Giamarchi, and P. Le Doussal, Phys. Rev. Lett. **80**, 849 (1998).

[2] P. J. Metaxas, J. P. Jamet, A. Mougin, M. Cormier, J. Ferré, V. Baltz, B. Rodmacq, B. Dieny, and R. L. Stamps, Phys. Rev. Lett. **99**, 217208 (2007).

[3] J. Ferré, P. J. Metaxas, A. Mougin, J.-P. Jamet, J. Gorchon, and V. Jeudy, C. R. Phys. **14**, 651 (2013).

[4] L. B. Ioffe and V. M. Vinokur, J. Phys. C **20**, 6149 (1987).

[5] T. Nattermann, Europhys. Lett. **4**, 1241 (1987).

[6] V. Jeudy, A. Mougin, S. Bustingorry, W. Savero Torres, J. Gorchon, A. B. Kolton, A. Lemaître, and J.-P. Jamet, Phys. Rev. Lett. **117**, 057201 (2016).

[7] P. Chauve, T. Giamarchi, and P. Le Doussal, Phys. Rev. B **62**, 6241 (2000).

[8] A. B. Kolton, A. Rosso, T. Giamarchi, and W. Krauth, Phys. Rev. Lett. **97**, 057001 (2006).

[9] A. B. Kolton, A. Rosso, T. Giamarchi, and W. Krauth, Phys. Rev. B **79**, 184207 (2009).

[10] E. E. Ferrero, S. Bustingorry, A. B. Kolton, and A. Rosso, C. R. Phys. **14**, 641 (2013).

[11] E. E. Ferrero, L. Foini, T. Giamarchi, A. B. Kolton, and A. Rosso, Phys. Rev. Lett. **118**, 147208 (2017).

[12] T. Nattermann, Y. Shapir, and I. Vilfan, Phys. Rev. B **42**, 8577 (1990).

[13] T. Tybell, P. Paruch, T. Giamarchi, and J.-M. Triscone, Phys. Rev. Lett. **89**, 097601 (2002).

[14] W. Kleemann, J. Rhensius, O. Petracic, J. Ferré, J. P. Jamet, and H. Bernas, Phys. Rev. Lett. **99**, 097203 (2007).

[15] P. Paruch and J. Guyonnet, C. R. Phys. **14**, 667 (2013).

[16] B. Ziegler, K. Martens, T. Giamarchi, and P. Paruch, Phys. Rev. Lett. **111**, 247604 (2013).

[17] P. Tückmantel, I. Gaponenko, N. Caballero, J. C. Agar, L. W. Martin, T. Giamarchi, and P. Paruch, Phys. Rev. Lett. **126**, 117601 (2021).

[18] G. Blatter, M. V. Feigel'man, V. B. Geshkenbein, A. I. Larkin, and V. M. Vinokur, Rev. Mod. Phys. **66**, 1125 (1994).

[19] T. Nattermann and S. Scheidl, Adv. Phys. **49**, 607 (2000).

[20] T. Giamarchi and P. Le Doussal, in *Spin Glasses and Random Fields* (World Scientific, Singapore, 1998), pp. 321–356.

[21] T. Giamarchi and S. Bhattacharya, in *High Magnetic Fields* (Springer, Berlin, 2002), pp. 314–360.

[22] W.-K. Kwok, U. Welp, A. Glatz, A. E. Koshelev, K. J. Kihlstrom, and G. W. Crabtree, Rep. Prog. Phys. **79**, 116501 (2016).

[23] S. Brazovskii and T. Nattermann, Adv. Phys. **53**, 177 (2004).

[24] L. Ponson, Phys. Rev. Lett. **103**, 055501 (2009).

[25] D. Bonamy and E. Bouchaud, Phys. Rep. **498**, 1 (2011).

[26] E. E. Ferrero, L. Foini, T. Giamarchi, A. B. Kolton, and A. Rosso, Annual Review of Condensed Matter Physics **12**, 111 (2021).

[27] J. Gorchon, S. Bustingorry, J. Ferré, V. Jeudy, A. B. Kolton, and T. Giamarchi, Phys. Rev. Lett. **113**, 027205 (2014).

[28] R. Diaz Pardo, W. Savero Torres, A. B. Kolton, S. Bustingorry, and V. Jeudy, Phys. Rev. B **95**, 184434 (2017).

[29] N. B. Caballero, I. Fernández Aguirre, L. J. Albornoz, A. B. Kolton, J. C. Rojas-Sánchez, S. Collin, J. M. George, R. Diaz Pardo, V. Jeudy, S. Bustingorry, and J. Curiale, Phys. Rev. B **96**, 224422 (2017).

[30] V. Jeudy, R. Díaz Pardo, W. Savero Torres, S. Bustingorry, and A. B. Kolton, Phys. Rev. B **98**, 054406 (2018).

[31] M. P. Grassi, A. B. Kolton, V. Jeudy, A. Mougin, S. Bustingorry, and J. Curiale, Phys. Rev. B **98**, 224201 (2018).

[32] W. S. Torres, R. D. Pardo, S. Bustingorry, A. B. Kolton, A. Lemaître, and V. Jeudy, Phys. Rev. B **99**, 201201(R) (2019).

[33] P. Domenichini, C. P. Quinteros, M. Granada, S. Collin, J.-M. George, J. Curiale, S. Bustingorry, M. G. Capeluto, and G. Pasquini, Phys. Rev. B **99**, 214401 (2019).

[34] M. Yamanouchi, J. Ieda, F. Matsukura, S. E. Barnes, S. Maekawa, and H. Ohno, Science **317**, 1726 (2007).

[35] J.-C. Lee, K.-J. Kim, J. Ryu, K.-W. Moon, S.-J. Yun, G.-H. Gim, K.-S. Lee, K.-H. Shin, H.-W. Lee, and S.-B. Choe, Phys. Rev. Lett. **107**, 067201 (2011).

[36] S. DuttaGupta, S. Fukami, C. Zhang, H. Sato, M. Yamanouchi, F. Matsukura, and H. Ohno, Nat. Phys. **12**, 333 (2016).

[37] L. Caretta, M. Mann, F. Büttner, K. Ueda, B. Pfau, C. M. Günther, P. Hessing, A. Churikova, C. Klose, M. Schneider, D. Engel, C. Marcus, D. Bono, K. Bagschik, S. Eisebitt, and G. S. D. Beach, Nat. Nanotechnol. **13**, 1154 (2018).

[38] R. Díaz Pardo, N. Moisan, L. J. Albornoz, A. Lemaître, J. Curiale, and V. Jeudy, Phys. Rev. B **100**, 184420 (2019).

[39] T. Nattermann, V. Pokrovsky, and V. M. Vinokur, Phys. Rev. Lett. **87**, 197005 (2001).

[40] A. Glatz, T. Nattermann, and V. Pokrovsky, Phys. Rev. Lett. **90**, 047201 (2003).

[41] A. Bray, Adv. Phys. **43**, 357 (1994).

[42] See for instance, B. White, in *Proceedings of the International Congress of Mathematicians, Beijing*, edited by L. I. Tatsien (LI Daqian) Vol. 1 (Higher Education Press, Beijing, 2002), pp. 525–538.

[43] See Ref. [30] for values of $H_d$, $T_d$ and also the associated fundamental Larkin length $L_d$ in different magnetic materials.

[44] Typical external fields $H_t$ applied in creep experiments induce DW motion that can be measured by PMOKE, whereas for $H_t = 0$, DW motion solely driven by the curvature effective field $C\kappa_t$ is hardly observed in typical experimental time scales and micrometer-sized domains, so for typical finite fields $H_t \gg C\kappa_t$. See [45] for more details.

[45] See Supplemental Material at http://link.aps.org/supplemental/10.1103/PhysRevB.103.L220409 for the details of the experimental setup and protocols as well as the analytical and numerical calculations. An experimental movie is also included.

[46] J.-C. Rojas-Sánchez, P. Laczkowski, J. Sampaio, S. Collin, K. Bouzehouane, N. Reyren, H. Jaffrès, A. Mougin, and J.-M. George, Appl. Phys. Lett. **108**, 082406 (2016).

[47] C. P. Quinteros, M. J. Cortés Burgos, L. J. Albornoz, J. E. Gómez, P. Granell, F. Golmar, M. L. Ibarra, S. Bustingorry, J. Curiale, and M. Granada, J. Phys. D **54**, 015002 (2021).

[48] N. B. Caballero, E. E. Ferrero, A. B. Kolton, J. Curiale, V. Jeudy, and S. Bustingorry, Phys. Rev. E **97**, 062122 (2018).

[49] N. Caballero, E. Agoritsas, V. Lecomte, and T. Giamarchi, Phys. Rev. B **102**, 104204 (2020).

[50] P. C. Guruciaga, N. B. Caballero, V. Jeudy, J. Curiale, and S. Bustingorry, J. Stat. Mech. (2021) 033211.

[51] N. Caballero, arXiv:2009.14205.

[52] Note that we do not attempt to simulate creep but the "depinning-like" dynamics which effectively emerges by coarse graining many creep events [7]. Although the time-dependent Ginzburg-Landau model with thermal noise has all the ingredients, the universal creep formula that we can observe experimentally has been so far numerically tested only in much simpler models which can be solved with algorithms able to overcome the ultraslow dynamics and high futility that characterize the deep universal creep regime [9].

[53] A. L. Barabási and H. E. Stanley, *Fractal Concepts in Surface Growth* (Cambridge University Press, Cambridge, 1995).

[54] For small number of cycles $N$, the DW position is found to be uni-valued in polar coordinates.
[55] Since the oscillatory motion is superimposed with a slow drift we cannot discard a crossover at large $N$ towards the Edwards-Wilkinson growth.
[56] See Ref. [45] Sec. VIII for estimates of domain collapse lifetimes.
[57] K.-W. Moon, J.-C. Lee, S.-G. Je, K.-S. Lee, K.-H. Shin, and S.-B. Choe, Appl. Phys. Express **4**, 043004 (2011).
[58] L. Herrera Diez, V. Jeudy, G. Durin, A. Casiraghi, Y. T. Liu, M. Voto, G. Agnus, D. Bouville, L. Vila, J. Langer, B. Ocker, L. Lopez-Diaz, and D. Ravelosona, Phys. Rev. B **98**, 054417 (2018).
[59] L. Herrera Diez, F. Ummelen, V. Jeudy, G. Durin, L. Lopez-Diaz, R. Diaz-Pardo, A. Casiraghi, G. Agnus, D. Bouville, J. Langer, B. Ocker, R. Lavrijsen, H. J. M. Swagten, and D. Ravelosona, Appl. Phys. Lett. **117**, 062406 (2020).
[60] W. Kleemann, Annu. Rev. Mater. Res. **37**, 415 (2007).